
Risks of uncertainty propagation in AI-augmented security pipelines

Emanuele Mezzi | Aurora Papotti | Fabio Massacci | Katja Tuma

¹Department of Computer Science, Foundational and Experimental Security, Vrije Universiteit Amsterdam, The Netherlands

Correspondence

Emanuele Mezzi, Department of Computer Science, Foundational and Experimental Security, Vrije Universiteit Amsterdam, Amsterdam
Email: e.mezzi@vu.nl

Abstract

The use of AI technologies is percolating into the secure development of software-based systems, with an increasing trend of composing AI-based subsystems (with uncertain levels of performance) into automated pipelines. This presents a fundamental research challenge and poses a serious threat to safety-critical domains (e.g., aviation). Despite the existing knowledge about uncertainty in risk analysis, no previous work has estimated the uncertainty of AI-augmented systems given the propagation of errors in the pipeline. We provide the formal underpinnings for capturing uncertainty propagation, develop a simulator to quantify uncertainty, and evaluate the simulation of propagating errors with two case studies. We discuss the generalizability of our approach and present policy implications and recommendations for aviation. Future work includes extending the approach and investigating the required metrics for validation in the aviation domain.

KEYWORDS

artificial intelligence, automatic program repair, uncertainty quantification

1 | INTRODUCTION

Due to the increasing availability of data, AI technologies have spread and are being used in almost every computing system, including in safety-critical domains like aviation (EASA, 2023a). Although the use of AI-augmented systems comes with new promises of improved performance, it also introduces significant risks and challenges (EASA, 2023b; Cox Jr, 2020; Nateghi & Aven, 2021). A major challenge in using AI for risk analysis is conveying to decision-makers the uncertainty inherent to predictions of models, because it clashes with the common practice in the realm of AI to communicate uncertainty with point estimates or ignoring it completely (Guikema, 2020).

With the rise of open-source software development and large-scale cloud deployment, more security risk decision-making is automated by running sequences of AI-augmented analyses, like automated program repair (APR) (Long et al., 2017; Ye et al., 2021; Li et al., 2022; Xia & Zhang, 2022; Fu et al., 2024). The use of AI in automated security pipelines, where the first classifier detects a vulnerability and the second tool fixes it, is now becoming more common (Bui et al., 2024), which brings about a fundamental research challenge:

Propagating uncertainty is the new major challenge for assessing the risk of automated security pipelines.

This foundational problem has already manifested in security pipelines with no AI-based computation. To illustrate this problem, we consider four studies: verifying the presence of code smells (Tufano et al., 2017), generalizing the SZZ algorithm to identify the past versions of software affected by a vulnerability (Dashevskiy et al., 2018), identifying vulnerabilities in Java libraries (Kula et al., 2018), and finding how vulnerable Android libraries could be automatically updated (Derr, 2017).

A few years later, Pashchenko et al. (2020) showed that the results by Kula et al. (2018) are incorrect, and Huang et al. (2019) found that the claims by Derr et al. (2017) are incorrect, both to a large extent. We argue that the reason for this mishap is foundational. All these studies share the impossibility of running manual validation and do not report the uncertainty of their outcomes. The proposed solutions process huge inputs (e.g., 246K commits in Dashevskiy et al. (2018)) so they need an automated tool (with an error rate) to decide whether each sample satisfies the property of interest.

With the appearance of new AI-based approaches, such as SeqTrans (Chi et al., 2022), it is becoming imperative to investigate this problem now, before it is too late and AI-augmented

Abbreviations: AI, Artificial Intelligence; APR, automatic program repair; ML, Machine Learning; DL, Deep Learning; TP, True Positive; FN, False Negative; TN, True Negative; FP, False Positive.

systems without global measures of risk become weaved into the automated pipelines in organizations.

To address these issues, we focus on understanding the uncertainty due to error propagation in AI Augmented Systems. Among the pipeline, each component may be a potential source of error that leads to an underestimation or overestimation of the actual effectiveness of the proposed solution. Therefore, we formulate the overarching research question:

RQ: *How to estimate the total error (or success rate) of the AI-augmented system, given the propagating errors of the classifiers in the pipeline?*

If analytical models for the classifiers and the fixer components existed, it could be possible to use the error propagation models used for calculus (Benke et al., 2018). Unfortunately, analytical models of the recall and precision of these tools are extremely rare, therefore, we must resort to the much coarse-grained approximation with probability bound analysis (PBA) (Iskandar, 2021).

1.1 | Contributions

We provide the formal underpinnings for capturing uncertainty propagation in AI-augmented APR pipelines. In addition, we develop a simulator to quantify the effects that propagating uncertainty has in automated APR tools (such as the one presented in Figure 1). We evaluate the simulator and present two case studies, in which we calculate the effects of uncertainty regarding two proposed solutions[‡]. Finally, we discuss the policy implications and recommendations for the aviation domain.

2 | BACKGROUND AND RELATED WORK

We illustrate the composition of AI-augmented APR tools as background and present the related work on uncertainty quantification in AI, and applications of AI to vulnerability detection and APR.

2.1 | AI-augmented systems

Figure 1, shows the simplest example of composed AI-augmented system in the area of APR. It is composed by (i) a classifier, which labels code samples as *Good* or *Bad* by detecting which sample is not vulnerable and which is vulnerable, (ii) a fixer tool to transform *Bad* samples into *Good* samples, (iii) and the second classifier, which can be either equal to the first

or different, which analyzes the samples modified by the fixer to check whether they have been successfully repaired. The outcome of the final step is what we call *claimed success rate* or *fix rate*, representing the ratio of fixed vulnerable samples. Here we list each step executed by the AI-augmented APR tool and the possible errors propagating from it:

- Step one: the first classifier analyzes the code samples, and labels each of them as *Good*, or *Bad*. If a code sample presents features not encoded in the distribution learnt by the classifier, misclassification is probable, and thus the possibility that a *Good* code sample is misclassified as *Bad* or vice-versa.
- Second step: the fixer tries to fix every *Bad* code sample, transforming it into a *Fixed* code sample. Here the possibility of error lies in the fixer's performance.
- Third step: the second classifier analyzes the *Fixed* code samples. This is the outcome of the entire system. The second classifier performs a final analysis to detect which applications have not been successfully fixed by the fixer. The possibility of errors lies in the same conditions defined for the first classifier.

In our research, we focus on the errors of the first and second classifiers, by modelling and propagating the uncertainty which characterises their capacity to spot vulnerable code, namely the *recall*.

2.2 | Uncertainty quantification in AI

Hüllermeier and Waegeman (2021), highlight two macro-categories of methods employed to quantify and manage uncertainty in Machine Learning (ML). The first discerns between frequentist-inspired and Bayesian-inspired quantification methods. The second considers the distinction between uncertainty quantification and set-values prediction. Uncertainty quantification methods allow the model to output the prediction and the paired level of certainty, while the set-value methods consist of pre-defining a desired level of certainty and producing a set of candidates that comply with it.

Abdar et al. 2021 centre their analysis on Deep Learning (DL). Bayesian-inspired methods and ensemble methods represent two of the major categories to represent uncertainty in DL. Through Bayesian methods the DL model samples its parameters from a learnt posterior distribution, allowing the model to avoid fixed parameters and allowing us to inspect the variance and uncover the uncertainty which surrounds the model predictions. The most common Bayesian-inspired technique is the Monte Carlo (MC) dropout. Ensemble methods, combine different predictions from different deterministic predictors. Although they were not introduced in the first instance to explicitly

[‡] Following the best practices of open science we plan to provide a replication package in the final version of the manuscript.

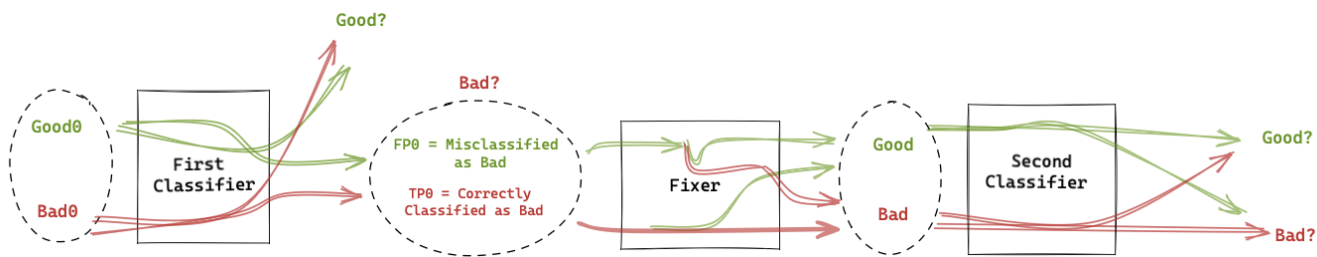


FIGURE 1 Illustration of an AI-augmented system which composes vulnerability detection and program repair. The first classifier receives in input the ground truth and determines which are the positive samples to be sent to the fixer to be repaired. The fixer, based on its effectiveness, tries to repair them. The second classifier checks whether the fixing is correct. We can also observe the errors made by each component of the pipeline. The first classifier can wrongly classify samples as positive when they are negative. The fixer can fail in repairing positive samples, and the second classifier can misclassify the samples received and that were modified by the fixer.

handle uncertainties, they give an intuitive way of representing the model uncertainty on a prediction by evaluating the variety among the predictors (Gawlikowski et al., 2023).

Key Observation 1

Extensive research was performed in the field of uncertainty quantification in AI, which brought the development of a variety of methods. However, these approaches are focused on uncertainty quantification of single models, without measuring the propagating effects of uncertainty about the output of the first model when piped as input into another part of the system.

2.3 | AI in vulnerability detection

Vulnerability detection is a crucial step in risk analysis of software systems and includes running automated tools scanning parts of the system to prevent future exploitation. Given its potential, experts integrated AI into their vulnerability detection systems, to scale them and make them more flexible to new threats.

One of the approaches to perform vulnerability detection is obtained by applying Natural Language Processing. In their approach, Hou et al. (2022), represent the code in the form of a syntax tree and input it to a Transformer model, which leverages the attention mechanism to improve the probability of detecting vulnerabilities. In their research, Akter et al. (2022), create embeddings using Glove and fastText and then use LSTM and Quantum LSTM models to perform vulnerability detection, showing lower execution time and higher accuracy, precision, and recall for the Quantum LSTM.

Another line of research excludes Natural Language Processing or embeds it with graph approaches. Yang et al. (2022),

propose a new code representation method called vulnerability dependence representation graph, allowing the embedding of the data dependence of the variables in the statements and the control structures corresponding to the statements. Moreover, they propose a graph learning network based on a heterogeneous graph transformer, which can automatically learn the importance of contextual sentences for vulnerable sentences. They carry out experiments on the SARD dataset with an improvement in performance between 4.1% and 62.7%. Fan et al. (2023), propose a circle gated graph neural network (CG-GNN) that receives an input tensor structure used to represent information of code. CGGNN possess the capacity to perform heterogeneous graph information fusion more directly and effectively and allows the researchers to reach a higher accuracy precision and recall compared to the TensorGNN and Devign methods. Finally, Zhang et al. (2023) propose Vul-GAI, to overcome the limitations posed by the training time in graph neural network models. They base their methods on graphs and images and unroll their approach in four phases: the graph generation from the code, the node embedding and the image generation from the node embedding. Then vulnerability detection through convolutional neural networks (CNN) is applied. VulGAI is tested on 40657 functions and overcomes the other methods VulDePecker, SySeVR, Devign, VulCNN, mVulPreter and, in accuracy, recall and f1-score also improved by 3.9 times the detection time of VulCNN.

Key Observation 2

Extensive research and different approaches were experimented with in the past, with a high level of performance.

However, previous work does not quantify (or communicate) the uncertainty regarding the performance of the proposed methods, and yet, the overestimated performance of the vulnerability detection model could affect the entire pipeline performance.

Key observation 3

Recently, substantial research has appeared regarding the automation of vulnerability fixing. These advances are important and could help to manage the manual effort spent on sieving through tool warnings. However, to the best of our knowledge, the propagation of errors (or final uncertainty of the result) has not been investigated in such automated pipelines.

2.4 | APR and composed pipelines

The step which follows automatic vulnerability detection through AI is the application of AI to automatic code fixing.

2.4.1 | Code fixers

Li et al. (2022) propose DEAR, a DL approach which supports fixing general bugs. Experiments run on three selected datasets: Defects4J (395 bugs), BigFix (+26k bugs), and CPat-Miner (+44k bugs) show that the DEAR approach outperforms existing baselines. Chi et al. (2022) leverage Neural Machine Translation (NMT) techniques, to provide a novel approach called SeqTrans to exploit historical vulnerability fixes to automatically fix the source code. Xia & Zhang (2022), propose AlphaRepair, which directly leverages large pre-trained code models for APR without any fine-tuning/retraining on historical bug fixes.

2.4.2 | Composed pipelines

AIBUGHUNTER combines vulnerability detection and code repair. The pipeline is implemented by Fu et al. (2024), combining LineVul (Fu & Tantithamthavorn, 2022) and VulRepair (Fu et al., 2022), two software implemented by the same author. Yang et al. (2020) propose a DL approach based on autoencoders and CNNs, automating bug localization and repairs. Another example of a complete pipeline combining vulnerability detection and code repair is HERCULES, which employs ML to fix code (Saha et al., 2019). Liu et al. (2021), evaluate the effect of fault localization by introducing the metric *fault localization sensitiveness* (*Sens*) and analysing 11 APR tools. *Sens*, is calculated with the ratio of plausibly fixed bugs by modifying the code on non-buggy positions, and the percentage of bugs which could be correctly fixed when the exact bug positions are available but cannot be found by the tool with its fault localization capacities. This metric, to the best of our knowledge, is the first to quantify the impact of the vulnerability detector capability on the overall pipeline. Nevertheless, it does not provide an interval to describe the best and worst pipeline performance, and thus the quantification of the risk in terms of the percentage of errors which the pipeline will overlook when it is employed.

3 | PIPELINE FORMALIZATION

In this section, we present the formal basis for our simulator. To simplify the analysis, we make the following assumptions in our model:

- *No breaking*: We assume that the fixer will never turn a true good sample that is classified as bad into a bad sample.
- *No degradation*: We assume that all elements that are fixed, cannot be distinguished from good elements from the beginning. In other words, the performance of the second classifier does not degrade with the fix.

3.1 | Identify the classifier metrics

To evaluate the goodness of the AI-augmented system we use the metrics which are typically used to report the performance of a classifier: True Positive Rate (*TPR*) or Recall (*rec*), precision (*prec*). We also use the prevalence rate (P_R) of the positive elements (*Pos*) among the total number of objects (N) in the domain of interest. The prevalence rate is not typically known, so we will assume it to be a parameter whose effects need to be explored by simulation. Specificity is rarely cited in publications using AI models and its absence makes it difficult to reverse engineer the True Negatives.

$$Pos = TP + FN \quad (1)$$

$$Neg = N - Pos \quad (2)$$

$$P_R = \frac{Pos}{N} \quad (3)$$

$$TPR = \frac{TP}{Pos} = rec = \frac{TP}{TP + FN} \quad (4)$$

$$FAR = \frac{FP}{Neg} = \frac{FP}{FP + TN} \quad (5)$$

$$prec = \frac{TP}{TP + FP} \quad (6)$$

For our purposes, it is more useful to express TP , FN and FP in terms of the other values that are often found in publications reporting results of AI-augmented system components.

Proposition 1. *Let rec be the recall of a classifier and $prec$ be its precision. When applied to a domain with N elements and a prevalence rate of P_R , the true positives TP , false negatives FN , and false positives FP of the classifier are as follows:*

$$TP = rec \cdot P_R \cdot N \quad (7)$$

$$FN = (1 - rec) \cdot P_R \cdot N \quad (8)$$

$$FP = rec \cdot \frac{1 - prec}{prec} \cdot P_R \cdot N \quad (9)$$

Proof. The first two equations are simply an inversion of the definition of recall (4), where positives Pos are expressed as a function of the prevalence rate (3). The third equation is obtained by inverting the definition of precision (6) to express false positives FP as a function of TP and $prec$ and then replace into it the equation computing TP as a function of recall rec and prevalence P_R (7). \square

3.2 | Deterministic recall, partial repairs, no breaking changes

Proposition 2. *Let rec be the recall rate of a classifier that is used both as a first and second classifier, let f_R be the theoretical fix rate of the fixer which (i) only affects positive (vulnerable) code and (ii) does not break nor make vulnerable code of the not vulnerable code which is eventually piped through it. The classifier can also correctly recognize unsatisfactory fixes (iii) with the same recall rec . Then the AI-augmented system true performance when applied to a domain with N elements and an initial prevalence rate of P_R , is*

$$f(aias) = f_R \cdot rec \quad (10)$$

$$P_R(aias) = (1 - f_R \cdot rec) \cdot P_R \quad (11)$$

$$TPR(aias) = rec \cdot \frac{(1 - f_R) \cdot rec}{1 - f_R \cdot rec} \quad (12)$$

$$FAR(aias) = rec^2 \cdot \frac{1 - prec}{prec} \cdot \frac{(1 - f_R) \cdot P_R}{1 - (1 - f_R \cdot rec) \cdot P_R} \quad (13)$$

The results, even under such favourable assumptions, are interesting as they show that uncertainty in the recall may change the overall expected fix rate. Further, it shows that, unless the fix rate is perfect, the prevalence rate is not reduced to zero and it will depend on the uncertainty in the recall.

An apparently surprising result is that if the fix rate is perfect then the overall true positive rate (TPR) is zero. This is actually to be expected: with a perfect fix rate, all identified positives are fixed. This does not mean that all positives are eliminated because the false negatives from the first classifier

are still present. In general, since $rec \leq 1$ we have that the term $\frac{(1 - f_R) \cdot rec}{1 - f_R \cdot rec} \leq 1$ and therefore the recall of the AI-augmented system as a whole is lower than the recall of the first classifier, i.e. $TPR(aias) \leq TPR$ (see Appendix, section A4).

While the recall of the AI-augmented system does not depend on the prevalence rate, the false alert rate (FAR) depends in a non-linear way on the overall prevalence rate of the system. It is still possible to prove that the false alert rate of the AI-augmented system as a whole is lower than the false alert rate of the first classifier, i.e. $FAR(aias) \leq FAR$.

Proof. 2 The first classifier receives in input the positives and the negatives and divides them into TP , FP , FN , and TN .

The fixer receives in input $TP_{1st} + FP_{1st}$ of which only a fraction f_R of TP_{1st} is actually fixed (Assumption (i)). According to assumption (ii) the fixer will not transform the false positive into new positives (i.e. it will not transform them into positives nor will not break them). Since the second instance of the classifier does not change the nature of the processed object but at worst misclassifies it we have that

$$Pos(aias) = \overbrace{(1 - f_R)TP_{1st}}^{\text{unfixed by fixer}} + \overbrace{FN_{1st}}^{\text{misclassified by 1st classifier}} \quad (14)$$

$$Pos(aias) = Pos - f(aias) \cdot Pos = P_R \cdot N - f(aias) \cdot P_R \cdot N \quad (15)$$

We now equates the terms, replace TP_{1st} and FN_{1st} with the corresponding equations, and simplify $P_R \cdot N$ from both sides of the equation to obtain $1 - f(aias) = (1 - f_R) \cdot rec + (1 - rec)$ which simplifies to $f(aias) = f_R \cdot rec$ (see Appendix, section A1).

We can use equation (15) to directly obtain the prevalence rate for the AI-augmented system by replacing the value of $f(aias)$ just computed and dividing by the total number of elements N .

To compute the true positive rate we replace in the definition of TPR (4) the number of TP surviving at the end of the second classifier which is $(1 - f_R) \cdot TP_{1st} \cdot rec$ because by assumption (ii) and (iii) only the original true positives will be reclassified as positives. We divide by the total number of positives of the AI-augmented system as computed from equation 15. By simplifying both numerator and denominator for $P_R \cdot N$ we obtain

$$TPR(aias) = \frac{(1 - f_R) \cdot rec \cdot rec}{1 - f_R \cdot rec} \quad (16)$$

To compute the false alert rate we need to compute first the false positives of the second classifier. To this extent, we rewrite the definition of false positives (9) in terms of the new set of positives $(1 - f_R)TP_{1st}$ at the end of the fixer according

to equation (14).

$$FP(aias) = rec \cdot \frac{1 - prec}{prec} \cdot (1 - f_R) \cdot rec \cdot P_R \cdot N \quad (17)$$

Then we substitute this value into the definition of the false alert rate (5) with the value of the overall negatives of the system. \square

Corollary 1. *Unless the fix rate is perfect ($f_R = 1$) the number of false negatives of the AI-augmented system satisfying the condition of Proposition 2 is higher than the number of false negatives that would result from just the first classifier. The false negatives of the AI-augmented system also increase with the increase in recall rec .*

This result is surprising as we expected the system to improve as recall improves. However, a larger recall would also mean that more positives would be piped through the fixer and tested again. Since the fixer is not perfect the number of false negatives emerging from the second run of the classifier will increase.

Proof. We compute the false negatives at the end of the AI-augmented system starting from the definition as

$$FN(aias) = \underbrace{\overbrace{[(1 - f_R) \cdot TP_{1st}]}}_{\text{unfixed positives}} \cdot \underbrace{(1 - rec)}_{\text{Escaping the 2nd classifier}} + FN_{1st} \quad (18)$$

We plug in the definition of TP_{1st} and FN_{1st} in terms of positives Pos and thus of the prevalence rate P_R and the overall number of objects N and re-arrange the terms to obtain

$$FN(aias) = [1 + (1 - f_R) \cdot rec] \cdot (1 - rec) \cdot P_R \cdot N \quad (19)$$

$$= [1 + (1 - f_R) \cdot rec] \cdot FN_{1st} \quad (20)$$

\square

By using the above equations we can compute the total number of elements which will be passed to the fixer and the second classifier.

$$N_{2nd} = TP_{1st} + FP_{1st} = \frac{rec}{prec} \cdot P_R \cdot N \quad (21)$$

By using assumption (iii) the positive that will be recognized as such $TP(aias)$ as

$$TP_{2nd} = \underbrace{\overbrace{(1 - f_R) \cdot TP_{1st}}}_{\text{unfixed positives}} \cdot \underbrace{rec}_{\text{after the second classifier}} \quad (22)$$

By expanding the definition of $TP_{1st} = rec \cdot Pos$ (7) and the definition of positives as $Pos = P_R \cdot N$ (1) and re-arranging the terms we have

$$TP(aias) = (1 - f_R) \cdot rec^2 \cdot P_R \cdot N \quad (23)$$

Then we can revise the final prevalence rate as

$$P_R(aias) = \frac{TP(aias) + FN(aias)}{TP(aias) + FN(aias) + TN(aias) + FP(aias)} \quad (24)$$

$$= \frac{TP(aias) + FN(aias)}{N}$$

We can plug the solution for $TP(aias)$ and $FN(aias)$ and observe that they are both multiplied by common factor $P_R \cdot N$ which allows us to simplify the denominator and remove the dependency by the total number of objects. The ratio between the final prevalence and the initial prevalence rate is then captured by the following expression:

$$\frac{P_R(aias)}{P_R} = (1 - f_R) \cdot rec^2 + [1 + (1 - f_R) \cdot rec] \cdot (1 - rec) \quad (25)$$

which further algebraically simplifies as follows:

$$P_R(aias) = (1 - f_R \cdot rec) \cdot P_R \quad (26)$$

By multiplying both ends by N we obtain the total number of positives before and after the treatment by the AI-augmented system pipeline. The AI-augmented system fix rate is therefore equal to

$$\frac{Pos - Pos(aias)}{Pos} = f_R \cdot rec \quad (27)$$

Complete derivations of $P_R(aias)$, $TPR(aias)$, and $FAR(aias)$, N_{2nd} , $FN(aias)$, $TP(aias)$, in sections A12, A3, A6, A8, A11, A10, in the Appendix.

3.3 | Uncertain recall

We employ PBA (Iskandar, 2021), to propagate, in the form of interval, uncertainty in the recall through the pipeline. By substituting a specific cumulative distribution function (CDF) with the p-boxes, PBA allows to model the lack of knowledge regarding the specific CDF from which the recall values are sampled. Considering that we cannot possess exhaustive information regarding the CDF of recalls of AI vulnerability detectors, the choice of this mathematical tool is preferred, compared for instance with probabilistic sensitivity analysis. Formulas 28 and 29, are the inverse p-boxes used to sample the lower and upper bound for the recall interval.

$$\underline{F}(p)_{a,b,\mu}^{-1} = \begin{cases} [a, \mu] & \text{for } p = 0 \\ \frac{p \cdot a - \mu}{p - 1} & \text{for } 0 < p < \frac{b - \mu}{b - a} \\ b & \text{for } \frac{b - \mu}{b - a} \leq p \leq 1 \end{cases} \quad (28)$$

$$\bar{F}(p)_{a,b,\mu}^{-1} = \begin{cases} a & \text{for } 0 \leq p \leq \frac{b-\mu}{b-a} \\ b - \frac{b-\mu}{p} & \text{for } \frac{b-\mu}{b-a} < p < 1 \\ [\mu, b] & \text{for } p = 1 \end{cases} \quad (29)$$

Thus the *rec* will now correspond to an interval of values:

$$recall = [\underline{rec}, \overline{rec}] \quad (30)$$

By substituting \underline{rec} and \overline{rec} , in Equations 26, 10, and 18, we can derive the lower and upper bound for $P_R(aias)$, $f(aias)$, and $FN(aias)$ thus quantifying the uncertainty characterising them:

$$P_R(aias) = [P_R(aias), \overline{P_R(aias)}] \quad (31)$$

$$f(aias) = [f(aias), \overline{f(aias)}] \quad (32)$$

$$FN(aias) = [FN(aias), \overline{FN(aias)}] \quad (33)$$

4 | RECALL IN THE FIELD

We collect the reported recall values (and precision) of AI-augmented vulnerability detectors and derive the parameters necessary to implement the p-boxes in our simulations.

4.1 | Search in digital libraries

Figure 2 illustrates the steps that define our search. We defined a search string to filter publications stored in digital libraries: (**"vulnerability detection" OR "fault localization"**) AND (**"artificial intelligence" OR "AI" OR "Deep Learning" OR "DL" OR "machine learning" OR "ML"**) AND (**"sensitivity" OR "true positive rate" OR "TPR" OR "recall" OR "hit rate"**) AND **"code"**.

We define a list of selection criteria (SC) that a publication must respect to be selected for the extraction of data points.

- SC1. The publication must be related to the topic of vulnerability detection or fault localization. For instance, we discard publications related to general *feature location*.
- SC2. The publication must apply ML or DL algorithms to the problem of vulnerability detection. We discard the publications which do not employ ML or DL.
- SC3. Since the metrics considered $P_R(aias)$, $f(aias)$, and $FN(aias)$, depend uniquely on the recall, the publication must (at least) report the recall of the vulnerability detectors.

We employed the search string on Scopus without filtering based on the time of publication. We process the 548 results

ordered by relevance. We consider the first 200 because they represent a sufficient sample size. After applying SC1 and SC2 to the title and abstract, we retain 142 publications. Finally, applying SC3 resulted in removing 27 more publications.

4.2 | Collected samples

After eliminating the outliers (30), there remain 2328 samples that we use to build the p-boxes. The minimum and maximum reported recall are respectively 0.07 and 1.00, while the mean is 0.74. For completeness in Table 1 we also show descriptive statistics on the collected precision samples (but we do not use them yet in our simulation).

TABLE 1 Descriptive statistics regarding the recall and precision data, gathered from publications related to the applications of AI to vulnerability detection.

Measure	Samples	Publications	Min	Max	Mean
Recall	2328	115	0.07	1.00	0.74
Precision	2043	100	0.00	1.00	0.71

5 | SIMULATION

Through the simulation, we are interested in calculating $P_R(aias)$, $f(aias)$, $FN(aias)$ which, as previously shown (Section 3), depend uniquely on the recall. To allow for future extensions, we implemented the simulator taking into account TN and FP , which are needed to define specificity. At this stage of the research, the specificity value does not affect the final result, thus we set its value to zero.

5.1 | Simulator

Figure 3 illustrates the subsystems of our simulation pipeline. It is composed of a fixer and a classifier which acts as the first and second classifiers.

5.1.1 | Ground truth generator

We use a ground truth generator to generate the dataset that allows the simulation of the pipeline. Each generated sample represents a code sample, which can be vulnerable or not vulnerable. Thus, the ground truth generator generates fictional positive and negative elements (*Pos*, *Neg*).

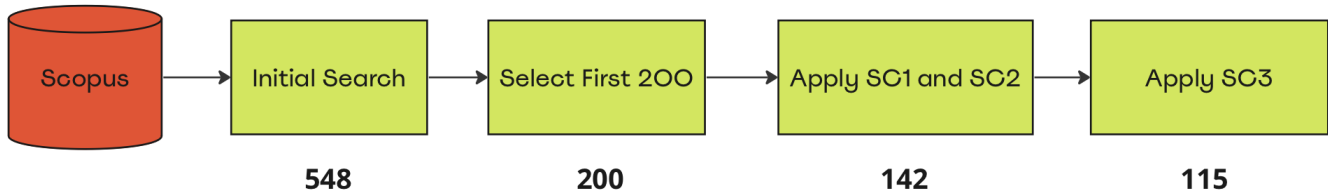


FIGURE 2 The figure shows the steps implemented to gather the publications from which to extract recall values. The first step consists of an initial search on Scopus that retrieves 548 publications. Based on the relevance, the first 200 are selected. We check which of these 200 publications implement vulnerability detection of fault localization, using AI. In the end, of the 142 publications that respect the previous conditions, we select only the ones which used recall as an evaluation metric.

- It receives as input the total number of elements (N), and the initial prevalence rate (P_R), which defines an initial number of vulnerable elements.
- The generator labels each object as vulnerable with probability equal to P_R , and not vulnerable with probability $1 - P_R$ and returns a list containing all the samples generated.

5.1.2 | P-boxes and recall sampling

We implement formulas 28 and 29 to sample from the p-boxes, and use them to sample N lower and upper bound recall values to run the simulations.

- Both implementations of Formulas 28 and 29 receive as input the minimum (0.07), maximum (1.00), and mean (0.74) value generated from the exploratory data analysis (Section 4.2), and a list of probability values sampled from a uniform distribution.
- For each of the uniform values, we sample lower and upper recall bounds. Given the two lists of recall values, one for the lower bound and one for the upper bound, each of N elements, we run N simulations that allow us to calculate the upper and lower bounds.

5.1.3 | First classifier

After generating the lower and upper bound recall values, the first classifier executes the first subdivision of the samples, generating TP_{1st} , FN_{1st} , TN_{1st} , and FP_{1st} .

- The first classifier discerns each vulnerable element of the ground truth between TP with probability equal to rec and as FN with probability equal to $1 - rec$. This means that the greater the recall the greater the probability that vulnerable objects are classified as TP .
- Since the first classifier is simulated with both lower and upper bound recall values, in the end, we obtain lower

and upper bounds for each element, thus $[TP_{1st}, \overline{TP_{1st}}]$, $[FN_{1st}, \overline{FN_{1st}}]$, $[TN_{1st}, \overline{TN_{1st}}]$, $[FP_{1st}, \overline{FP_{1st}}]$.

5.1.4 | Fixer

The fixer, with fix rate f_R , tries to repair the samples classified as positives by the first classifier, namely TP_{1st} and FP_{1st} . The fixer repairs each sample classified as positive with probability equal to f_R . Since we assume that a FP cannot be broken, the intervention on FP cannot cause it to become a TP .

5.1.5 | Second classifier

The second classifier, with the same recall and specificity as the first classifier, classifies the objects that passed through the fixer, generating TP_{2nd} , FN_{2nd} , TN_{2nd} , and FP_{2nd} .

- The second classifier labels each vulnerable object that passed through the fixer as TP with probability equal to the rec and as FN with probability $1 - rec$.
- Since the second classifier is simulated with both lower and upper bound recall values, we obtain lower and upper bounds for each element, thus $[TP_{2nd}, \overline{TP_{2nd}}]$, $[FN_{2nd}, \overline{FN_{2nd}}]$, $[TN_{2nd}, \overline{TN_{2nd}}]$, and $[FP_{2nd}, \overline{FP_{2nd}}]$.

5.1.6 | Final counter

The final counter gathers the results from the first classifier, the fixer, and the second classifier and that calculates the final prevalence rate ($P_R(aias)$), the final fix rate ($f(aias)$), and the ratio (FN_{ratio}) between the final number of false negatives ($FN(aias)$) and the false negatives generated by the first classifier (FN_{1st}). Since the uncertainty propagates until the final counter, each metric will be characterised by a lower and upper bound, thus: $[P_R(aias), \overline{P_R(aias)}]$, $[f(aias), \overline{f(aias)}]$, $[FN_{ratio}, \overline{FN_{ratio}}]$.

The code to reproduce the ground truth generator, the p-boxes formulas and recall sampling, the first classifier, the fixer, the

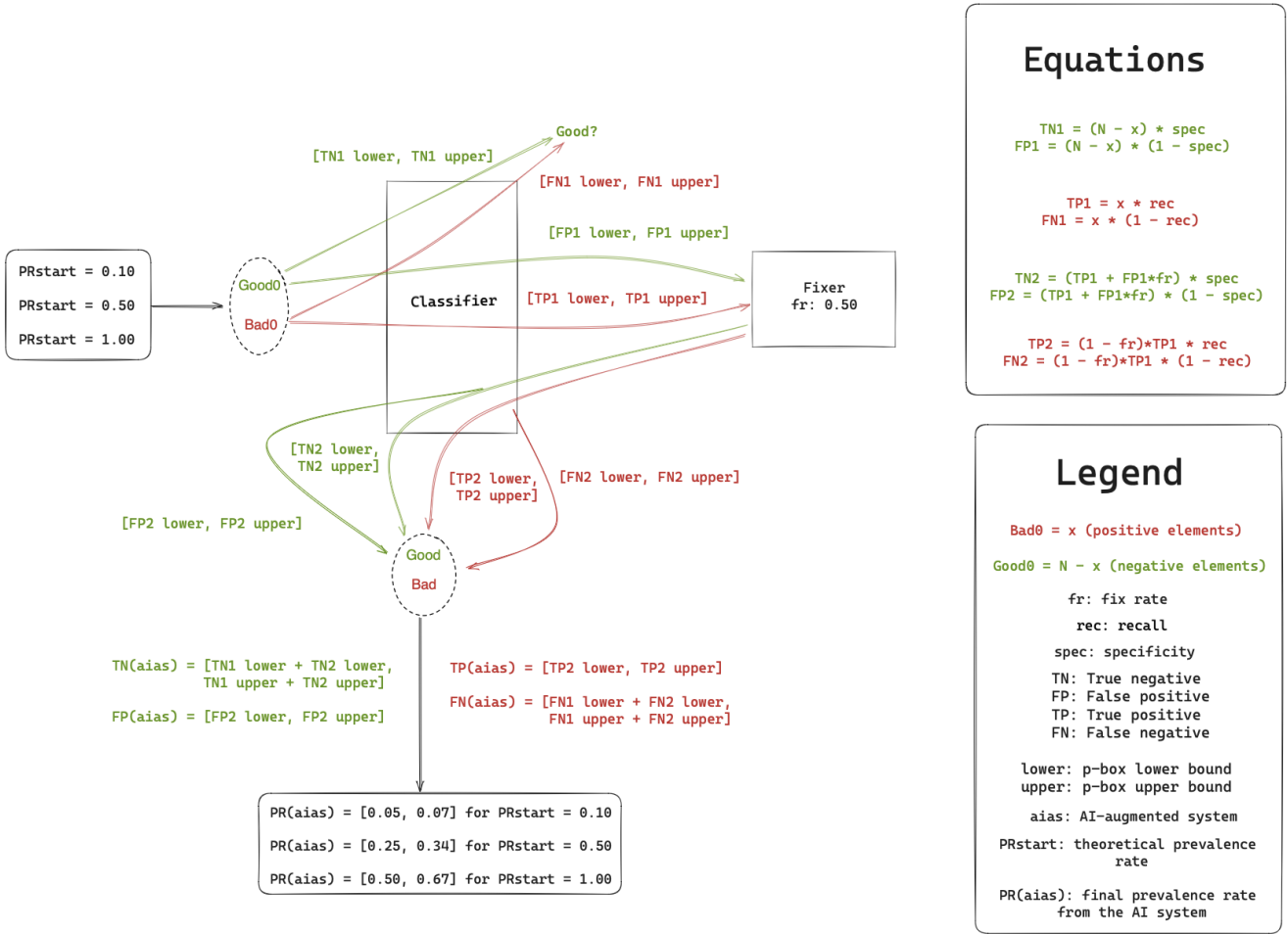


FIGURE 3 Illustration of the process that leads to the calculation of the final prevalence rate ($P_R(\text{aias})$), given a fixed rate of 0.50 and three different starting prevalence rates (P_R). P_R determines the number of positives in the ground truth, while $P_R(\text{aias})$ is the ratio between the positives ($TP(\text{aias}) + FN(\text{aias})$) and the total elements (N) at the end of the process. We represent the pipeline in the form of a loop because the first and the second classifiers possess the same recall and specificity. By considering at each step in the pipeline, a lower and upper bound of the recall, we propagate the uncertainty, with the consequence that also the $P_R(\text{aias})$, as TP , FN , TN , and FP , will have an upper and lower bound. The lower bound of the $P_R(\text{aias})$ is the best-case scenario, which is the case in which the classifier is perfect. In reality, $P_R(\text{aias})$ can be equal to all the values contained in the interval, depending on the classifier's performance.

second classifier, and the counter, can be found in the Appendix, respectively in sections B1, B2, B3, B4, B5, B6.

5.2 | Simulation results

We present the simulation results and show how propagating uncertainty affects $P_R(\text{aias})$ (see Table 2), $f(\text{aias})$ (see Table 3), and the false negatives (see Table 4). Figure 3 instantiates the simulated pipeline, with the results obtained from one of the simulations.

5.2.1 | Final prevalence rate

Table 2 shows the results related to the decrease in the prevalence rate. We run simulations with $P_R = (0.10, 0.50, 1.00)$, thus in the first, second and third sets of simulation, the total number of vulnerable samples is equal to the 10%, 50% and 100% of the total samples. For each of these simulation sets, we calculate the final prevalence rate with $f_R = (0.50, 0.70, 0.90, 1.00)$, meaning that the expected decrease in the prevalence rate is respectively 50%, 70%, 90% and 100%. But, the theoretical decrease in the prevalence rate that should be observed given a specific starting prevalence rate and fix rate,

is only the lower bound of the interval, which corresponds to the minimum prevalence rate obtainable when the capacity to locate vulnerable elements is perfect. In all the other cases the value will fall within the bounds of the interval. For example, when $P_R = 0.50$ and $f_R = 0.50$ we should observe a decrease in the final prevalence rate of 50%, thus $P_R(aias) = 0.25$. But, Table 2 and Figure 3 show that the 50% decrease only represents the lower bound, contrasting with an upper bound of 0.34.

TABLE 2 This table shows how the bounds of the final prevalence rate ($\mathbf{P}_R(\mathbf{aias})$) given initial prevalence rate (\mathbf{P}_R), and theoretical fix rate (\mathbf{f}_R), but uncertain recall. The theoretical decrease of the initial prevalence rate given a fix rate only consists of the lower bound of the interval. For instance when $\mathbf{P}_R = 1.00$ and $\mathbf{f}_R = 0.50$, the prevalence rate decreases of the 50% but only as a lower bound. The upper bound of the final prevalence rate is equal to 0.67.

\mathbf{P}_R	$\mathbf{P}_R(\mathbf{aias})$			
	$\mathbf{f}_R = 0.50$	$\mathbf{f}_R = 0.70$	$\mathbf{f}_R = 0.90$	$\mathbf{f}_R = 1.00$
0.10	[0.05, 0.07]	[0.03, 0.05]	[0.00, 0.04]	[0.00, 0.03]
0.50	[0.25, 0.34]	[0.15, 0.27]	[0.05, 0.20]	[0.00, 0.17]
1.00	[0.50, 0.67]	[0.30, 0.54]	[0.11, 0.40]	[0.01, 0.33]

5.2.2 | Real fix rate

Table 3 show the results related to the final fix rate. We run simulations with theoretical fix rate $f_R = (0.50, 0.70, 0.90, 1.00)$. At the end of the simulations, f_R only corresponds to the upper bound of the interval of $f(\mathbf{aias})$, which is the maximum fix rate obtainable when the capacity to locate vulnerable elements is maximum. For example, when $f_R = 0.50$, the $f(\mathbf{aias})$ oscillates between a maximum of 0.50 equal to f_R and a minimum of 0.03. This illustrates the limitations of APR tools and the importance of stating the final results in terms of intervals and not of single numbers, to represent the uncertainty that characterises these systems when they are applied to real-world scenarios.

TABLE 3 Comparison between the theoretical fix rate (\mathbf{f}_R) and the real fix rate ($\mathbf{f}(\mathbf{aias})$). The theoretical fix rate, only translates into the upper bound of the interval, while the real fix rate can fall within a much wider range of values, which will eventually depend on the quality of the classifier.

\mathbf{f}_R	$\mathbf{f}(\mathbf{aias})$
0.50	[0.03, 0.50]
0.70	[0.05, 0.70]
0.90	[0.06, 0.90]
1.00	[0.07, 1.00]

5.2.3 | False negatives ratio

Table 4 shows the results related to FN_{ratio} , which is the ratio between the false negatives generated by the first classifier FN_{1st} and the overall number of false negatives registered at the end of the pipeline $FN(\mathbf{aias})$. Apart for $f_R = 1$, the final ratio is always greater than one, and this indicates that the pipeline is unable to avoid the growth of the number of FN between the first and the second classifier.

TABLE 4 This table shows the final bounds regarding the ratio (\mathbf{FN}_{ratio}). Between the first and the second classifier, the number of FN grows apart in the case in which the $\mathbf{f}_R = 1$. When the $\mathbf{f}_R = 1$, $\mathbf{FN}(\mathbf{aias}) = \mathbf{FN}_{1st}$, because there will be no positives that can be classified as FN by the second classifier and thus the number will not increase, leaving the ratio equal to one.

\mathbf{f}_R	\mathbf{FN}_{ratio}
0.50	[1.37, 1.38]
0.70	[1.22, 1.23]
0.90	[1.07, 1.07]
1.00	[1.00, 1.00]

6 | CASE STUDIES

We present two case studies, that measure the impact of uncertainty on rule-based and AI-based APR tools.

6.1 | Case study one: rule-based APR

The case study concerning rule-based APR tools is derived from the research by Liu et al. (2020). In this publication performances of 16 APR tools are tested on the dataset Defects4J, which is composed of 395 elements and thus allows for manual validation. Since every element in the dataset is vulnerable, of the total number of code samples, the number of elements which the first classifiers consider positive is 395. The number of bugs repaired changes from tool to tool, but considering the best tool, namely ACS, the number of Fixed code samples is 16, while the number of non-fixed bugs is 379.

We use this case study to show how uncertainty deriving from possible errors during manual validation, can impact the results conveyed in the form of points estimates, which do not account for possible errors. As suggested by Dashevskiy et al. (2018), we employ the Agresti-Coull-Wilson confidence interval analysis (Agresti & Coull, 1998), which is a method to construct an accurate and reliable confidence interval, also

for small samples sized, and that we use to generate an upper and lower bound regarding the percentage of correct generated patches. Table 5, shows the impact of the uncertainty on the tools that have the best and the worst performance expressed in terms of patches that can fix bugs. Using a 95% confidence interval the esteems for the percentage of correct patches vary widely, both for the three best tools and for the three worst.

TABLE 5 The first three columns are derived from Liu et al. (2020) and report the generated patches on the reference dataset Defects4J for each APR Tool and the patches that are semantically correct. In the last two columns, we show the 95% confidence interval of the potential error rate for the corresponding tool based on the Agresti-Coull-Wilson confidence interval analysis. For example, ACS reported 16 repaired bugs but the correct patches might be between 51.13% and 72.7%. For the DynaMoth, a tool such as correct patches might be as low as 0.00%.

Tool	Reported (Liu et al., 2020)		C.I. Error 95%	
	# Repaired	CR(%)	Lower	Upper
ACS	16 (22)	72.7%	51.13%	87.33%
SimFix	25 (68)	36.8%	26.09%	48.91%
FixMiner	12 (33)	36.4%	21.89%	53.78%
Kali-A	3 (65)	4.6%	1.00%	13.49%
DynaMoth	1 (22)	4.5%	0.00%	24.07%
Nopol	1 (31)	3.2%	0.00%	18.04%

6.2 | Case study two: AI-based APR

This case study examines the possibility of obtaining an AI-augmented APR tool, composed of two AI subsystems, one dedicated to vulnerability detection, and the other to vulnerability repair.

We analyze a DL-based APR tool, AIBUGHUNTER (Fu et al., 2024). This pipeline is the result of the assembly of two systems, namely LineVul (Fu & Tantithamthavorn, 2022), which performs vulnerability detection and VulRepair (Fu et al., 2022), which performs bug-fixing. Since the authors specified that they did not evaluate the whole AIBUGHUNTER pipeline in the dedicated publication, but that they evaluated the two composing tools separately, we use this case study to show to what extent uncertainty can impact the overall performance of an APR pipeline composed by different AI subsystems, trained on different datasets. We consider the dataset on which AIBUGHUNTER is tested, composed of 879 total code samples, all of which have vulnerabilities. We calculate the number of the samples that the first classifier of the pipeline highlights to be vulnerable by multiplying the total code samples by the recall reported in the publication dedicated to LineVul (Fu & Tantithamthavorn, 2022) which amounts to 0.86, obtaining 756

Bad code samples. Then, VulRepair (Fu et al., 2022), with a reported repairing accuracy of 0.44 is used to correct the bugs. Thus we multiply the repairing accuracy by the number of Bad code samples, obtaining 333 Fixed code samples. Thus the number of positive elements which the pipeline does not correct is equal to 423. We then use our simulation pipeline to account for uncertainty in the recall, considering the same number of code samples and the same point estimate for repairing accuracy. Once we account for uncertainty, the final repairing accuracy could be as high as 0.47, but as low as 0.03, compared to the starting point estimate of 0.44.

7 | DISCUSSION

7.1 | Summary of results

Simulation results show that, once the uncertainty in the recall of the vulnerability detectors is propagated through the pipeline, it affects the overall pipeline performance, in terms of prevalence rate reduction and real fix rate. The simulated AI system can obtain the expected theoretical reduction of the prevalence rate, and a final fix rate equal to the theoretical fix rate, only in the best-case scenario, which is when the recall is maximum. In all the other cases, the real reduction of the number of vulnerable code samples, and the final fix rate, can widely vary, falling in the intervals calculated during the simulation. This finding was confirmed when investigating case studies. While the first case study shows that uncertainty can impact scenarios where AI is not involved, the second case study confirms that the final fix rate depends on the oscillation of the classifier recall.

Second, our simulations show that the uncertainty characterising the FN_{ratio} is smaller compared to the uncertainty characterising $P_R(aias)$ and $f(aias)$. That is the difference between the lower and upper bound of the intervals related to the FN_{ratio} is smaller compared to the intervals of $P_R(aias)$ and $f(aias)$. However, the incapacity of the pipeline to keep the FN stable between the first and the second classifier could mean overlooking true vulnerabilities due to over-approximation of classifier performance, which could lead to untrustworthy decisions about security risks exposing the possible discrepancy between the preference of risk managers who use the AI system, and the risk tolerance embedded in the system (Paté-Cornell, 2024).

Answer to RQ

How to estimate the total error (or success rate) of the AI-augmented system, given the propagating errors of the classifiers in the pipeline?

We propose an approach to assess the risk of propagating uncertainty based on the propagation of the recall in a security pipeline. We implement the pipeline through simulation and show the final intervals for $P_R(aias)$, $f(aias)$, and FN_{ratio} . We use our pipeline to evaluate the potential propagation of uncertainty with case studies, showing that in some cases (case study two), although the $f_R = 0.44$, it could be as low as 0.03 once uncertainty is considered using our approach.

7.2 | Policy and recommendations for aviation

The necessity to consider uncertainty at the system level has implications for the policies to be adopted in scenarios where AI is applied to safety-risk systems such as in the case of aviation. Although the European Union Aviation Safety Agency (EASA) (2023a; 2023b), highlights the potential of AI applied to cybersecurity and the importance of uncertainty quantification, two major gaps still exist:

- Vulnerability detection and patching systems: while EASA (2023a) highlights the possible use of AI to detect vulnerabilities and correct code, the scope of the analysis is for now limited to addressing the attacks to which ML systems can be subject to (EASA, 2023b). To date, no guidelines have been published concerning APR tools in the field of cybersecurity for aviation.
- Subsystem focus: in the realm of safety assessment and information security, which constitute two important building blocks of the trustworthy AI framework defined by EASA, and of which the first include uncertainty management, the objectives to be reached are characterised at subsystem level (EASA, 2023b):

Objective SA-01: The applicant should perform a safety (support) assessment for all AI-based **(sub)systems**, identifying and addressing specificities introduced by AI/ML usage.

Objective IS-01: For each AI-based **(sub)system** and its data sets, the applicant should identify those information security risks with an impact on safety, identifying and addressing specific threats introduced by AI/ML usage.

Contrasting with the EASA approach, our results, related to APR tools but whose implications can be extended also to other AI-augmented systems, highlight the importance of modelling uncertainty at the system level, propagating it from the singular subsystems that compose the entire pipeline, to verify how

the entanglement of the uncertainties of the different components affects the entire system. Thus, to improve the guidelines, we advise dedicating a section to describe the guidelines that will be needed to implement AI-augmented APR tools to be employed in aviation and to further emphasize the importance of quantifying uncertainty at the system level, when assessing safety and security.

7.3 | Limitations

7.3.1 | No-breaking assumption

In our research, we assume that the fixer cannot break the samples that the first classifier classifies as positive when they are negative. Since this is a simplification because we cannot assume that the fixer is perfect and cannot break the code, in future studies we will remove this assumption by experimenting with the breaking-possibility scenario.

7.3.2 | No-degradation assumption

We assume that all elements that are fixed, cannot be distinguished from good elements from the beginning. The performance of the classifier does not degrade with the fix. We are assuming that the fixer generates code within the same distribution of the originals that are analyzed by the first classifier, thus allowing us to use a second classifier equal to the first. The plan is to use two different classifiers in the future.

7.3.3 | Generalization of simulator to real systems

While we assume that the simulation is realistic as it is rooted in relevant theory and recall values reported in related work, we are not working with a real system. In the next step of our research, we will experiment with an actual pipeline, accounting for uncertainty and checking to what extent the results obtained during the simulation are reflected in an actual system.

8 | CONCLUSIONS

In practice, good performance of APR tools is still challenging to achieve. In a recent publication, Ami et al. (2023) surveyed 89 practitioners who use automated security testing, and one participant summarized the rate of false positives in reality:

“(At present) 80% of them are actually false positives and 20% of them are actually something we can fix.”

In addition, the lack of assessing the risk of introducing false negatives into the system is the bigger concern (Ami et al., 2023), which brings challenges for AI-based APR adoption:

“If the tools miss something, we can not detect that issue, and we just overlook the issues ...because no one ever reports about false negatives, and we don’t check if the tool ever misses the vulnerabilities”.

We presented a new approach for assessing the risk of uncertainty propagation and showed, by simulation, that the final performance of an AI-augmented system may be an entire order of magnitude lower (0.44 vs 0.03) when estimating the effect of propagating errors. Our simulations of the level of uncertainty are in line with the recall values reported in the related work. In addition, the modular implementation of the simulator allows domain experts to use an internal or alternative dataset of recall values, to approximate p-boxes and run a more precise, domain-specific simulation of the propagating uncertainty in their systems. This would allow them to make more informed security risk decisions.

However, future work is needed to validate to what extent the proposed simulation is perceived as useful and how practitioners interpret the communicated uncertainty. For instance, a validation could test whether other factors, connected to real-world and real-time scenarios, such as network traffic and limited bandwidth, or human factors, affect the system’s global uncertainty. Beyond the scenarios modelled in this work, it is worth considering how errors propagate in cases when the fixer modifies a misclassified sample, potentially introducing new vulnerabilities. Moreover, it is worth considering scenarios where the fixer introduces changes with patterns different from the ones that the first classifier is trained to recognize, as it can happen when the classifier and the fixer are trained on different datasets (Fu et al., 2024), as is often the case, as organizations adopt technologies based on their needs. Capturing these scenarios would allow policymakers to assess when model retraining is required and quantify the drop in residual uncertainty in their systems. Finally, more policy effort is required in aviation to guide risk assessments concerning APR tools in the field of cybersecurity for aviation, and error propagation from (sub)systems to the system level.

REFERENCES

- Abdar, M., Pourpanah, F., Hussain, S., Rezazadegan, D., Liu, L., Ghavamzadeh, M., ... Saeid, N. (2021). A review of uncertainty quantification in deep learning: Techniques, applications and challenges. *Information fusion*, 76, 243–297.
- Agresti, A., & Coull, B. A. (1998). Approximate is better than “exact” for interval estimation of binomial proportions. *The American Statistician*, 52(2), 119–126.
- Akter, M. S., Shahriar, H., & Bhuiya, Z. A. (2022). Automated vulnerability detection in source code using quantum natural language processing. In *International conference on ubiquitous security* (pp. 83–102).
- Ami, A. S., Moran, K., Poshyvanyk, D., & Nadkarni, A. (2023). “false negative-that one is going to kill you.”-understanding industry perspectives of static analysis based security testing. In *2024 IEEE Symposium on Security and Privacy (SP)* (pp. 19–19).
- Benke, K., Norng, S., Robinson, N., Benke, L., & Peterson, T. (2018). Error propagation in computer models: analytic approaches, advantages, disadvantages and constraints. *Stochastic Environmental Research and Risk Assessment*, 32, 2971–2985.
- Bui, Q.-C., Paramitha, R., Vu, D.-L., Massacci, F., & Scandariato, R. (2024). Apr4vul: an empirical study of automatic program repair techniques on real-world java vulnerabilities. *Empirical software engineering*, 29(1), 18.
- Chi, J., Qu, Y., Liu, T., Zheng, Q., & Yin, H. (2022). Seqtrans: automatic vulnerability fix via sequence to sequence learning. *IEEE Transactions on Software Engineering*, 49(2), 564–585.
- Cox Jr, L. A. (2020). Answerable and unanswerable questions in risk analysis with open-world novelty. *Risk Analysis*, 40(S1), 2144–2177.
- Dashevskiy, S., Brucker, A. D., & Massacci, F. (2018). A screening test for disclosed vulnerabilities in foss components. *IEEE Transactions on Software Engineering*, 45(10), 945–966.
- Derr, E., Bugiel, S., Fahl, S., Acar, Y., & Backes, M. (2017). Keep me updated: An empirical study of third-party library updatability on android. In *Proceedings of the 2017 ACM SIGSAC conference on computer and communications security* (pp. 2187–2200).
- EASA. (2023a). Easa artificial intelligence roadmap 2.0 [white paper]. EASA. <https://www.easa.europa.eu/en/downloads/137919/en>
- EASA. (2023b). Easa concept paper: First usable guidance for level 1&2 machine learning applications [white paper]. EASA. <https://www.easa.europa.eu/en/downloads/137631/en>
- Fan, Y., Wan, C., Fu, C., Han, L., & Xu, H. (2023). Vdotr: Vulnerability detection based on tensor representation of comprehensive code graphs. *Computers & Security*, 130, 103247.
- Fu, M., & Tantithamthavorn, C. (2022). Linevul: A transformer-based line-level vulnerability prediction. In *Proceedings of the 19th international conference on mining software repositories* (pp. 608–620).
- Fu, M., Tantithamthavorn, C., Le, T., Kume, Y., Nguyen, V., Phung, D., & Grundy, J. (2024). Aibughunter: A practical tool for predicting, classifying and repairing software vulnerabilities. *Empirical Software Engineering*, 29(1), 4.

- Fu, M., Tantithamthavorn, C., Le, T., Nguyen, V., & Phung, D. (2022). Vulrepair: a t5-based automated software vulnerability repair. In *Proceedings of the 30th acm joint european software engineering conference and symposium on the foundations of software engineering* (pp. 935–947).
- Gawlikowski, J., Tassi, C. R. N., Ali, M., Lee, J., Humt, M., Feng, J., ... Zhu, X. X. (2023). A survey of uncertainty in deep neural networks. *Artificial Intelligence Review*, 56(Suppl 1), 1513–1589.
- Guikema, S. (2020). Artificial intelligence for natural hazards risk analysis: Potential, challenges, and research needs. *Risk Analysis*, 40(6), 1117–1123.
- Hou, F., Zhou, K., Li, L., Tian, Y., Li, J., & Li, J. (2022). A vulnerability detection algorithm based on transformer model. In *International conference on artificial intelligence and security* (pp. 43–55).
- Huang, J., Borges, N., Bugiel, S., & Backes, M. (2019). Up-to-crash: Evaluating third-party library updatability on android. In *2019 ieee european symposium on security and privacy (euros&p)* (pp. 15–30).
- Hüllermeier, E., & Waegeman, W. (2021). Aleatoric and epistemic uncertainty in machine learning: An introduction to concepts and methods. *Machine Learning*, 110, 457–506.
- Iskandar, R. (2021). Probability bound analysis: A novel approach for quantifying parameter uncertainty in decision-analytic modeling and cost-effectiveness analysis. *Statistics in Medicine*, 40(29), 6501–6522.
- Kula, R. G., German, D. M., Ouni, A., Ishio, T., & Inoue, K. (2018). Do developers update their library dependencies? an empirical study on the impact of security advisories on library migration. *Empirical Software Engineering*, 23, 384–417.
- Li, Y., Wang, S., & Nguyen, T. N. (2022). Dear: A novel deep learning-based approach for automated program repair. In *Proceedings of the 44th international conference on software engineering* (pp. 511–523).
- Liu, K., Li, L., Koyuncu, A., Kim, D., Liu, Z., Klein, J., & Bissyandé, T. F. (2021). A critical review on the evaluation of automated program repair systems. *Journal of Systems and Software*, 171, 110817.
- Liu, K., Wang, S., Koyuncu, A., Kim, K., Bissyandé, T. F., Kim, D., ... Traon, Y. L. (2020). On the efficiency of test suite based program repair: A systematic assessment of 16 automated repair systems for java programs. In *Proceedings of the acm/ieee 42nd international conference on software engineering* (pp. 615–627).
- Long, F., Amidon, P., & Rinard, M. (2017). Automatic inference of code transforms for patch generation. In *Proceedings of the 2017 11th joint meeting on foundations of software engineering* (pp. 727–739).
- Nateghi, R., & Aven, T. (2021). Risk analysis in the age of big data: The promises and pitfalls. *Risk analysis*, 41(10), 1751–1758.
- Pashchenko, I., et al. (2020). Vuln4real: A methodology for counting actually vulnerable dependencies.
- Paté-Cornell, E. (2024). Preferences in ai algorithms: The need for relevant risk attitudes in automated decisions under uncertainties. *Risk Analysis*.
- Saha, S., et al. (2019). Harnessing evolution for multi-hunk program repair. In *2019 ieee/acm 41st international conference on software engineering (icse)* (pp. 13–24).
- Tufano, M., Palomba, F., Bavota, G., Oliveto, R., Di Penta, M., De Lucia, A., & Poshyvanyk, D. (2017). When and why your code starts to smell bad (and whether the smells go away). *IEEE Transactions on Software Engineering*, 43(11), 1063–1088.
- Xia, C. S., & Zhang, L. (2022). Less training, more repairing please: revisiting automated program repair via zero-shot learning. In *Proceedings of the 30th acm joint european software engineering conference and symposium on the foundations of software engineering* (pp. 959–971).
- Yang, G., Min, K., & Lee, B. (2020). Applying deep learning algorithm to automatic bug localization and repair. In *Proceedings of the 35th annual acm symposium on applied computing* (pp. 1634–1641).
- Yang, H., Yang, H., & Zhang, L. (2022). Vdght: A source code vulnerability detection method based on heterogeneous graph transformer. In *International symposium on cyberspace safety and security* (pp. 217–224).
- Ye, H., et al. (2021). Automated patch assessment for program repair at scale. , 26(2), 1–38.
- Zhang, C., & Xin, Y. (2023). Vulgai: vulnerability detection based on graphs and images. *Computers & Security*, 135, 103501.

Appendix

A | FORMULA DERIVATIONS

A1 | Derivation of AI-augmented system fix rate from the positives

$$Pos(aias) = (1 - f_R) \cdot TP_{1st} + FN_{1st} \quad (A1)$$

$$Pos(aias) = Pos - f(aias) \cdot Pos \quad (A2)$$

$$P_R \cdot N - f(aias) \cdot P_R \cdot N = (1 - f_R) \cdot rec \cdot P_R \cdot N + (1 - rec) \cdot P_R \cdot N \quad (A3)$$

$$1 - f(aias) = (1 - f_R) \cdot rec + (1 - rec) \quad (A4)$$

$$f(aias) = 1 - (1 - f_R) \cdot rec - (1 - rec) \quad (A5)$$

$$= 1 - rec + f_R \cdot rec - (1 - rec) \quad (A6)$$

$$= f_R \cdot rec \quad (A7)$$

A2 | Derivation of $P_R(aias)$ from $Pos(aias)$

$$Pos(aias) = Pos - f(aias) \cdot Pos \quad (A8)$$

$$P_R(aias) \cdot N = P_R \cdot N - f_R \cdot rec \cdot P_R \cdot N \quad (A9)$$

$$P_R(aias) = (1 - f_R \cdot rec) \cdot P_R \quad (A10)$$

A3 | Derivation of $TPR(aias)$

$$TPR(aias) = \frac{TP_{2nd}}{Pos(aias)} \quad (A11)$$

$$= \frac{(1 - f_R) \cdot TP_{1st} \cdot rec}{Pos - f(aias) \cdot Pos} \quad (A12)$$

$$= \frac{(1 - f_R) \cdot rec \cdot P_R \cdot N \cdot rec}{P_R \cdot N - f_R \cdot rec \cdot P_R \cdot N} \quad (A13)$$

$$= \frac{(1 - f_R) \cdot rec \cdot rec}{1 - f_R \cdot rec} \quad (A14)$$

A4 | $TPR(aias) \leq TPR$

$$\frac{(1 - f_R) \cdot rec}{1 - f_R \cdot rec} \leq 1 \quad (A15)$$

$$(1 - f_R) \cdot rec \leq 1 - f_R \cdot rec \quad (A16)$$

$$rec - f_R \cdot rec \geq 1 - f_R \cdot rec \quad (A17)$$

$$rec \geq 1 \quad (A18)$$

A5 | Derivation of the false positives

$$FP(aias) = rec \cdot \frac{1 - prec}{prec} \cdot (1 - f_R) \cdot rec \cdot P_R \cdot N \quad (A19)$$

A6 | Derivation of the FAR(aias)

$$FAR(aias) = \frac{FP(aias)}{Neg(aias)} = \frac{FP(aias)}{N - Pos(aias)} \quad (A20)$$

$$= \frac{rec \cdot \frac{1-prec}{prec} \cdot (1-f_R) \cdot rec \cdot P_R \cdot N}{N - (P_R \cdot N - f(aias) \cdot P_R \cdot N)} \quad (A21)$$

$$= \frac{rec \cdot \frac{1-prec}{prec} \cdot (1-f_R) \cdot rec \cdot P_R}{1 - (P_R - f_R \cdot rec) \cdot P_R} \quad (A22)$$

$$= rec \cdot \frac{1-prec}{prec} \frac{(1-f_R) \cdot rec \cdot P_R}{1 - (1-f_R \cdot rec) \cdot P_R} \quad (A23)$$

$$= rec^2 \cdot \frac{1-prec}{prec} \frac{(1-f_R) \cdot P_R}{1 - (1-f_R \cdot rec) \cdot P_R} \quad (A24)$$

A7 | Proof that the AI-augmented system false alert rate is less than or equal to the false alert rate of the first classifier ($FAR(aias) \leq FAR$)

$$FAR(aias) \leq FAR \quad (A25)$$

$$rec^2 \cdot \frac{1-prec}{prec} \frac{(1-f_R) \cdot P_R}{1 - (1-f_R \cdot rec) \cdot P_R} \leq rec \cdot \frac{1-prec}{prec} \frac{P_R \cdot N}{N - P_R \cdot N} \quad (A26)$$

$$rec \cdot \frac{(1-f_R) \cdot P_R}{1 - (1-f_R \cdot rec) \cdot P_R} \leq \frac{P_R}{1 - P_R} \quad (A27)$$

$$rec \cdot \frac{(1-f_R)}{1 - (1-f_R \cdot rec) \cdot P_R} \leq \frac{1}{1 - P_R} \quad (A28)$$

$$rec \cdot (1-f_R)(1 - P_R) \leq 1 - (1-f_R \cdot rec) \cdot P_R \quad (A29)$$

$$rec \cdot (1-f_R - P_R + f_R \cdot P_R) \leq 1 - P_R + f_R \cdot rec \cdot P_R \quad (A30)$$

$$rec - rec \cdot f_R - rec \cdot P_R + rec \cdot f_R \cdot P_R \leq 1 - P_R + f_R \cdot rec \cdot P_R \quad (A31)$$

$$rec - rec \cdot f_R - rec \cdot P_R \leq 1 - P_R \quad (A32)$$

$$rec \cdot (1 - f_R - P_R) \leq 1 - P_R \quad (A33)$$

$$\text{if } 1 - f_R - P_R > 0 \text{ which is } 1 > f_R + P_R \quad (A34)$$

$$rec \leq \frac{1 - P_R}{1 - f_R - P_R} \text{ and } 1 - f_R - P_R \leq 1 - P_R \text{ implies } 1 \leq \frac{1 - P_R}{1 - f_R - P_R} \quad (A35)$$

$$rec \leq 1 \leq \frac{1 - P_R}{1 - f_R - P_R} \text{ always true} \quad (A36)$$

$$\text{if } 1 - f_R - P_R < 0 \text{ which is } 1 < f_R + P_R \quad (A37)$$

$$rec \geq \frac{P_R - 1}{f_R + P_R - 1} \text{ and } P_R - 1 \geq 0 \text{ implies } \frac{P_R - 1}{f_R + P_R - 1} \geq 0 \quad (A38)$$

$$rec \geq 0 \geq \frac{P_R - 1}{f_R + P_R - 1} \text{ always true} \quad (A39)$$

A8 | Derivation of the total number of elements passed to the fixer

$$N_{2\text{nd}} = TP_{1\text{st}} + FP_{1\text{st}} \quad (\text{A40})$$

$$= rec \cdot P_R \cdot N + rec \cdot \frac{1 - prec}{prec} \cdot P_R \cdot N \quad (\text{A41})$$

$$= \frac{prec \cdot rec + rec - rec \cdot prec}{prec} \cdot P_R \cdot N \quad (\text{A42})$$

$$= \frac{rec}{prec} \cdot P_R \cdot N \quad (\text{A43})$$

A9 | Derivation of the false positives starting from the precision

$$prec = \frac{TP}{TP + FP} \quad (\text{A44})$$

$$(TP + FP) \cdot prec = TP \quad (\text{A45})$$

$$FP \cdot prec = TP \cdot (1 - prec) \quad (\text{A46})$$

$$FP = Pos \cdot rec \cdot \frac{1 - prec}{prec} \quad (\text{A47})$$

A10 | Derivation of the final number of true positives

$$TP(aias) = (1 - f_R) \cdot TP_{1\text{st}} \cdot rec \quad (\text{A48})$$

$$= (1 - f_R) \cdot (Pos \cdot rec) \cdot rec \quad (\text{A49})$$

$$= (1 - f_R) \cdot rec^2 \cdot Pos \quad (\text{A50})$$

$$= (1 - f_R) \cdot rec^2 \cdot P_R \cdot N \quad (\text{A51})$$

A11 | Derivation of the AI-augmented system false negatives (FN(aias))

$$FN(aias) = [(1 - f_R) \cdot TP_{1\text{st}}] \cdot (1 - rec) + FN_{1\text{st}} \quad (\text{A52})$$

$$= [(1 - f_R) \cdot (Pos \cdot rec)] \cdot (1 - rec) + (Pos \cdot (1 - rec)) \quad (\text{A53})$$

$$= \{[(1 - f_R) \cdot rec] \cdot (1 - rec) + (1 - rec)\} \cdot Pos \quad (\text{A54})$$

$$= \{[(1 - f_R) \cdot rec] + 1\} \cdot (1 - rec) \cdot Pos \quad (\text{A55})$$

$$= [1 + (1 - f_R) \cdot rec] \cdot (1 - rec) \cdot P_R \cdot N \quad (\text{A56})$$

$$= [1 + (1 - f_R) \cdot rec] \cdot FN_{1\text{st}} \quad (\text{A57})$$

A12 | Derivation of the AI-augmented system prevalence rate ($P_R(\text{aias})$)

$$P_R(\text{aias}) = \frac{TP(\text{aias}) + FN(\text{aias})}{TP(\text{aias}) + FN(\text{aias}) + TN(\text{aias}) + FP(\text{aias})} \quad (\text{A58})$$

$$= \frac{TP(\text{aias}) + FN(\text{aias})}{N} \quad (\text{A59})$$

$$= \frac{(1-f_R) \cdot rec^2 \cdot P_R \cdot N + [1 + (1-f_R) \cdot rec] \cdot (1-rec) \cdot P_R \cdot N}{N} \quad (\text{A60})$$

$$= (1-f_R) \cdot rec^2 \cdot P_R + [1 + (1-f_R) \cdot rec] \cdot (1-rec) \cdot P_R \quad (\text{A61})$$

$$= [(1-f_R) \cdot rec^2 + [1 + (1-f_R) \cdot rec] \cdot (1-rec)] \cdot P_R \quad (\text{A62})$$

$$= [(1-f_R) \cdot rec^2 + (1-rec) + (1-f_R) \cdot rec \cdot (1-rec)] \cdot P_R \quad (\text{A63})$$

$$= [(1-f_R) \cdot rec^2 + (1-rec) + (1-f_R) \cdot rec - (1-f_R) \cdot rec^2] \cdot P_R \quad (\text{A64})$$

$$= [1-rec + rec - f_R \cdot rec] \cdot P_R \quad (\text{A65})$$

$$= [1-f_R \cdot rec] \cdot P_R \quad (\text{A66})$$

B | CODE FOR SIMULATION

B1 | Code for the ground truth generator

LISTING 1 Code to reproduce the generation of the ground truth.

```
def ground_truth(work_rate, prev_rate, num_obj)
    vulnerable = 0
    not_vulnerable = 0
    ground_array = []

    for i in num_obj:
        random_vuln = random_uniform()
        random_work = random_uniform()

        if random_vuln > vuln_rate:
            vuln = 0
            not_vulnerable = not_vulnerable + 1
        else:
            vuln = 1
            vulnerable = vulnerable + 1

        if random_work > work_rate:
            work = 0
        else:
            work = 1

        ground_array.add("id": i, "vuln": vuln, "work": work)

    return ground_array
```

B2 | Code for inverse p-boxes and recall sampling

LISTING 2 Code to reproduce the p-boxes formulas used to quantify uncertainty.

```
def inverse_pbox_lower(a, b, loc, p_list)
    x_list = []

    for p in p_list:
        if p == 0:
            val = random_uniform(a, loc)
            x_list.add(val)
```

```

elif 0 < p < (b-loc)/(b-a):
    val = (p * a - loc) / (p - 1)
    x_list.add(val)
elif b - loc <= p <= 1:
    val = b
    x_list.add(val)

return x_list

def inverse_pbox_upper(a, b, loc, p_list)
    x_list = []

    for p in p_list do:
        if 0 <= p <= (b - loc) / (b - a):
            val = a
            x_list.add(val)
        elif (b - loc)/(b - a) < p < 1:
            val = b - (b - loc) / p
            x_list.add(val)
        elif p == 1:
            val = random_uniform(loc, b)
            x_list.add(val)

    return x_list

```

LISTING 3 Code that calls the lower and upper bound inverse p-box functions and generates lower and upper bound recall values.

```

p_list = stats.uniform.rvs(loc=0, scale=1, size=N, random_state=Y)

recall_lower_bound = inverse_p_box_lower_a_b_loc(min(recall), max(recall), mean(recall), p_list)
recall_upper_bound = inverse_p_box_upper_a_b_loc(min(recall), max(recall), mean(recall), p_list)

```

B3 | Code for first classifier

LISTING 4 Code to reproduce the operation of the first classifier.

```

def first_classifier(ground_array, recall, specificity)
    tp1, fp1, tn1, fn1 = 0, 0, 0, 0
    first_array = []

    for obj in ground_array:
        rec = random_uniform()
        spec = random_uniform()
        id_, vuln, work = obj[0], obj[1], obj[2]

        if vuln == 1:
            if rec <= recall:
                # Add a TP to first_array
                tp1 = tp1 + 1
            else:
                # Add a FN to first_array
                fn1 = fn1 + 1
        elif vuln == 0:
            if spec <= specificity:
                # Add a TN to first_array
                tn1 = tn1 + 1
            else:
                # Add a FP to first_array
                fp1 = fp1 + 1

    return first_array, tp1, fp1, tn1, fn1

```

B4 | Code for fixer

LISTING 5 Code to reproduce the operations of the fixer.

```
def fixer(first_array, f_rate, b_rate)
    fixer_array = []

    for obj in first_array:
        r_f = random_uniform()
        r_b = random_uniform()
        id_, vuln, work, class_ = obj[0], obj[1], obj[2], obj[3]

        if class_ == 1:
            if r_f <= f_rate and r_b <= b_rate:
                # Add a fixed, broken object to
                # fixer_array
            elif r_f <= f_rate and r_b > b_rate:
                # Add fixed, not broken object to
                # fixer_array
            elif r_f > f_rate and r_b > b_rate:
                # Add a not fixed, not broken object to
                # fixer_array
            elif r_f > f_rate and r_b <= b_rate:
                # Add not fixed, broken object to
                # fixer_array
        elif class_ == 0:
            # Add to fixer_array, the object that did not pass through the fixer

    return fixer_array
```

B5 | Code for second classifier

LISTING 6 Code to reproduce the operations of the second classifier.

```
def second_classifier(fixer_array, recall, specificity)
    tp2, fp2, tn2, fn2 = 0, 0, 0, 0
    second_array = []

    for obj in fixer_array:
        rec = random_uniform()
        spec = random_uniform()
        id_, vuln, work = obj[0], obj[1], obj[2]
        class_, fix = obj[3], obj[4]

        if fix == 'yes':
            if vuln == 1:
                if rec <= recall:
                    # Add a TP to second_array
                    tp2 = tp2 + 1
                else:
                    # Add a FN to second array
                    fn2 = fn2 + 1
            elif vuln == 0:
                if spec <= specificity:
                    # Add a TN to second_array
                    tn2 = tn2 + 1
                else:
                    # Add a FP to second_array
                    fp2 = fp2 + 1

        elif fix == 'no':
            # Add an object that did not pass
            # through the fixer to second_array

    return second_array, tp2, fp2, tn2, fn2
```

B6 | Code for final counter

LISTING 7 Code to reproduce the final calculation of the metrics.

```
def counter(ground_array, rec_spec_array)
    for (rec, spec) in rec_spec_array:
        for fix_rate in fix_rate values:
            for break_rate in break_rate values:
                first_array, tp1, fp1, fn1 = first_analyzer(ground_array, rec, spec)
                fixer_array = fixer(first_array, fix_rate, break_rate)
                second_array, tp2, fp2, tn2, fn2 = second_classifier(fixer_array, rec, spec)

                tp_out = tp2
                fp_out = fp2
                tn_out = tn1 + tn2
                fn_out = fn1 + fn2

                N = tp_out + fn_out + tn_out + fp_out
                final_pr = (tp_out + fn_out) / N
                pr_div = final_pr / first_pr
                real_fix_rate = 1 - prev_rate_div
                fn_div = fn_out / fn1

    return final_pr, pr_div, real_fix_rate, fn_div
```
